



 Cite this: *RSC Adv.*, 2026, 16, 1789

# Multifunctional performance of deep eutectic solvent (DES) $K_2CO_3$ –glycerol in biodiesel synthesis and purification

 Leily Nurul Komariah,<sup>a</sup>  <sup>\*</sup> Susila Arita,<sup>a</sup> Muhammad Daffa Khairuddin,<sup>b</sup> Siti Alifah Ovindirani,<sup>b</sup> Desi Erisna<sup>b</sup> and Tsabita Nayaka Paramasyifa<sup>c</sup>

Deep Eutectic Solvent  $K_2CO_3$ –Glycerol (DES K–G) was tested for its multiple roles in biodiesel production, serving as a catalyst, co-catalyst/reaction medium, and solvent in product purification. DES K–G was synthesised through a thermal mixing method at 80 °C with a molar ratio of  $K_2CO_3$ : glycerol = 1 : 3.5. The catalyst performance in transesterification occurred at 65 °C, stirring at 450 rpm, with a methanol to oil weight ratio of 30 wt%. Under the same process conditions and catalyst ratio (1.2% w/w), the reaction performance with DES K–G was comparable with that of Sodium Methylate (SMO). The standard quality parameters used as benchmarks are total glycerol (<0.24%) and methyl ester content (>96.5%). To achieve the standards, the reaction with DES K–G requires a reaction time of 4 h, while with SMO it takes 1.5 h. Furthermore, biodiesel synthesis was tested using a dual catalyst system, with a combination of DES K–G and SMO, at a weight ratio of 1 : 3, which demonstrated the highest methyl ester content of 98.256% within 2 h. DES K–G also showed the best impurity removal performance in a 2-cycle washing treatment. The combination of extraction with DES K–G in the first cycle, followed by water washing in the second cycle, provided the best separation efficiency. There was an increase in methyl ester content of 5.1%, followed by changes in density, saponification value, and acid value, respectively, of 1.15%, 14.3%, and 47.6%. Thus, DES K–G demonstrates versatility and great potential for integrated biodiesel synthesis and purification.

 Received 4th December 2025  
 Accepted 24th December 2025

DOI: 10.1039/d5ra09382a

[rsc.li/rsc-advances](http://rsc.li/rsc-advances)

## 1 Introduction

Biodiesel is the most popular bioenergy commodity in Indonesia. Its production and consumption have been progressively rising. Due to its widespread availability, palm oil or fats derived from it are used as raw materials in most biodiesel manufacturing plants in this country. Recently, the government has ambitiously targeted the use of a 50% biodiesel blend in various sectors, particularly the transportation sector. This programme is known as the B50 mandate.

Domestic biodiesel production continues to grow, and it has become a significant driver of glycerol as a by-product in recent years.<sup>1</sup> As another consequence, this increases the demand for catalysts. Meanwhile, currently, most catalysts for biodiesel production are still imported from abroad.

Conventional biodiesel production routes continue to rely on catalytic transesterification reactions involving methanol with

homogeneous catalysts.<sup>2,3</sup> The catalyst loading is typically in the range of 1–2% of the raw oil material's weight. The types of catalysts commonly used for commercial biodiesel production are sodium or potassium methylate. The significant advantage of these catalysts is the virtually water-free character, which results in higher yields, lower purification costs and more consistent biodiesel quality.<sup>4–6</sup>

Under certain conditions, a dual catalyst or the addition of a co-solvent is applied to improve reaction efficiency and accelerate the transesterification reaction. The type of co-solvent or reaction medium depends on the condition of the raw material, the process condition, and the catalyst used.<sup>7,8</sup>

Biodiesel purification is essential to remove contaminants such as residual methanol, soap, catalyst, free glycerine, and other impurities that may compromise the quality of the final product. Wet washing is the most traditional and widely used method for purifying biodiesel. It involves using water to remove impurities such as unreacted catalysts, alcohol, soaps, and other contaminants. Water can eliminate the remaining sodium salts and prevent the formation of soaps due to its solubility.<sup>9,10</sup> Traditional water washing commonly generates 0.5 to 10 litres of wastewater per liter of biodiesel.<sup>11</sup> Moreover, the use of water in biodiesel purification may lead to increased wastewater discharges, resulting in significant environmental

<sup>a</sup>Department of Chemical Engineering, Faculty of Engineering, Universitas Sriwijaya, Indralaya, South Sumatera, 30662, Indonesia. E-mail: leilynurul@unsri.ac.id

<sup>b</sup>Laboratory of Energy and Waste Treatment, Faculty of Engineering, Universitas Sriwijaya, Indralaya, South Sumatera, 30662, Indonesia

<sup>c</sup>Mathematical and Physical Science, Faculty of Arts and Science, University of Toronto, Ontario, M5S3G3, Canada


consequences.<sup>12</sup> Therefore, many methods are offered to overcome it, one of which is solvent washing or liquid–liquid extraction.

Solvents commonly used for purification include methanol/ethanol, hexane, heptane, *etc.* One of the challenges of using solvents in biodiesel washing is that some contain hazardous substances, posing a risk to the environment when released into liquid waste. Therefore, it is essential to select solvents that are not only selective for impurity removal but also environmentally friendly.

## 2 Deep eutectic solvents

Deep Eutectic Solvent (DES) is a mixture of two or more components in a specific molar ratio, which forms a eutectic mixture through hydrogen bonding. The formation of DES is characterised by a drastic decrease in melting point, forming a liquid at room temperature. The decrease in the melting point of the eutectic mixture occurs due to the strong interaction between the Hydrogen Bond Acceptor (HBA) anion and the Hydrogen Bond Donor (HBD) complexing agent.<sup>13–15</sup>

Recently, DES considered as low-cost alternative solvents. It has been suggested and widely used in both of the research works and industrial applications. The DES potential has received a lot of attention as an environmentally friendly solvent, non-toxic, biodegradable, and easy synthesis.<sup>16</sup>

DES is generally synthesised through thermal mixing, specifically heating and stirring methods. This procedure involves mixing two or more components at high temperatures to form a eutectic mixture. In practice, these solutions are prepared by directly adding the appropriate amounts of HBD and salt into a flask.

The components of DES interact with each other to form hydrogen bonds. Hydrogen bond interactions cause the melting point of DES to be lower than the melting points of its constituent components.<sup>14,17</sup> According to Martins *et al.*,<sup>18</sup> a mixture can be called DES if it has a lower melting point than its ideal eutectic temperature, thus differing from ordinary mixtures. The hydrogen bonding in DES forms a dynamic network, which can disrupt the original hydrogen-bonding patterns of proteins and form new non-covalent interactions.<sup>19</sup>

## 3 DES K<sub>2</sub>CO<sub>3</sub>–glycerol

In this study, K<sub>2</sub>CO<sub>3</sub> and glycerol were used as constituents of DES due to their abundant availability and low cost. Both components are non-toxic, renewable, and compatible with the principles of green chemistry.

Glycerol is a polyhydric alcohol compound consisting of three hydroxyl groups, so it is considered a strong hydrogen-bond donor. Glycerol is highly polar and viscous, so it promotes stable interactions. Its polarity supports the solvation and stabilization of ionic species in DES. Glycerol molecules form a strong and dense hydrogen-bond network, which can stabilize the DES. Potassium carbonate (K<sub>2</sub>CO<sub>3</sub>) is an inorganic chemical compound consisting of potassium ions (K<sup>+</sup>) and carbonate ions (CO<sub>3</sub><sup>2-</sup>). Potassium carbonate is alkaline, and

K<sub>2</sub>CO<sub>3</sub> provides catalytic basicity and increases the rate of transesterification in the biodiesel production.<sup>20,21</sup>

K<sub>2</sub>CO<sub>3</sub> was once used as a catalyst in the production of FAME through transesterification, as reported by several authors.<sup>22–24</sup> Rui Shan *et al.*<sup>25</sup> specifically conducted palm oil transesterification at 65 °C. They reported that loading K<sub>2</sub>CO<sub>3</sub> at 40 wt% exhibited the highest catalytic activity, yielding a biodiesel yield of 97.0%. Meanwhile, at the same catalyst ratio, Salmasi *et al.*<sup>26</sup> also achieved the highest yield of biodiesel (98.4%) in the transesterification of sunflower oil operated at 338 K with a reaction time of 4 hours. It shows that K<sub>2</sub>CO<sub>3</sub> salts in their single form can catalyze the reaction of fat/oil when operated at a higher ratio and with extended reaction time.

K<sub>2</sub>CO<sub>3</sub> and glycerol were selected as DES constituents because glycerol, a biodiesel-derived polyol, acts as an effective hydrogen-bond donor, while K<sub>2</sub>CO<sub>3</sub> provides strong basic hydrogen-bond-accepting carbonate species that generate catalytic activity. The combination forms a thermally stable eutectic liquid with high polarity and conductivity, enabling simultaneous functions as a reaction medium, base catalyst, and purification solvent.

Several characteristics provided by DES such as phase transition behaviour, solubility, and miscibility with reactants, and possesses acidity and basicity, which qualify them to be used in biodiesel synthesis.<sup>27–29</sup>

The use of DES from various constituents in the biodiesel production process is generally employed to enhance process efficiency and make the biodiesel production process more economical. Many researchers have tested DES derived from various constituents and successfully applied them as catalysts in transesterification processes,<sup>30–34</sup> interesterification<sup>35</sup> and esterification.<sup>36</sup> Several researchers have also demonstrated the ability of DES from various bases as solvents for biodiesel purification.<sup>37–40</sup> Specifically, DES K–G (DES K–G) has been tested by several researchers to improve the quality of biodiesel products, as compiled in Table 1.

According to Meng *et al.*,<sup>35</sup> hydrogen bonds are formed between the alcohol hydroxyl group and the carbonate ion, and this interaction activates the hydroxyl oxygen. In addition, the coordination of carbonyl groups with metal ions during the reaction makes the oxygen of the activated hydroxyl group more favourable to attack the positive carbon of the carbonyl group, thus triggering the reaction more efficiently (Table 2).<sup>16,41</sup>

### 3.1 Biodiesel purification using DES K–G

DES K–G not only exhibited catalytic reliability but also reduced side reactions, such as saponification in the transesterification reaction, enabling a straightforward biodiesel separation and purification.<sup>42</sup> The presence of hydroxyl groups in both DES K–G as a solvent and crude glycerol (CB) provides solvation power for glycerol in biodiesel. Additionally, DESs exhibit a high affinity for attracting glycerol through hydrogen bonding and dipole–dipole interactions.<sup>37</sup>

DES K–G has dual polarity characteristics. It exhibits strong hydrogen bonding due to glycerol (HBD) and basic/ionic interactions due to K<sub>2</sub>CO<sub>3</sub> (HBA). The combination creates a polar,



Table 1 Application of glycerol based DES in the reaction of biodiesel production

Role	Application	Process description	Results	Ref.
Catalyst	Transesterification of palm oil	Ratio $K_2CO_3$ : glycerol = 1 : 3.5, catalyst loading 4 wt%, methanol 30 wt%, 65–95 °C, 4 h	Methyl ester purity = 96.5%	31
Catalyst	Transesterification of <i>Jatropha curcas</i>	Molar ratio K : G = 1 : 32, catalyst loading = 8.96%, temperature = 60 °C, 70 min	Yield = 98.22%	47
Catalyst	Transesterification of rapeseed oil	Choline chloride : glycerol (1 : 2), catalyst: CaO, loading = 8.07 wt%, DES loading = 10.74 wt%	Yield = 91.9%	48
Co-catalyst	Transesterification of rapeseed oil	DES glycerol–ChCl, catalyst: NaOH 1.34 wt%, DES (co-catalyst) = 9.27 wt%	Mixing effectivity (DES–methanol–NaOH), yield = 98%	42
Reaction medium	Ethanolysis, dual catalyst	Lecithin–glycerol based-DES molar ratio of 1 : 2, loading 20 wt%, catalyst CaO 10%	DES accelerated the reaction	34
Reaction medium	Transesterification of rapeseed oil	Soybean oil, alcohol, $K_2CO_3$ and ionic liquid	Yield of biodiesel > 98%	41

hydrophilic phase that can selectively extract polar impurities from biodiesel. On the other hand, DES does not mix significantly with the nonpolar FAME phase.

The washing or extraction mechanism using DES mainly involves strong hydrogen bonding interactions between the solvent components (hydrogen bond donors and acceptors) and target compounds. It facilitates enhanced solvation, allowing DES to dissolve and extract poorly water-soluble molecules efficiently.

The tunable polarity of DES enables selective extraction based on compound characteristics, while DES can also physically and chemically disrupt cell walls or matrices, improving the release of embedded substances.

Controlled water content adjusts viscosity to facilitate better mass transfer during extraction without disrupting the

hydrogen bond network. Additionally, DES stabilizes extracted compounds, protecting them from degradation. Extraction efficiency may be further enhanced by techniques like ultrasound or microwave-assisted extraction, combined with the use of DES. An effective purification process should reduce the acid value to a level close to the standards for biodiesel fuel. Meanwhile, density is used as an indirect measure of purity and biodiesel composition. Properly purified biodiesel has a density within the specified standard range (0.86 to 0.89 g mL<sup>-1</sup>). Deviations from the normal range of density can indicate the presence of residual methanol, glycerol, water, or unreacted triglycerides.

DES molecules form hydrogen bonds with polar components in biodiesel, including MG, DG, FFA, and bioactive

Table 2 Application of glycerol based DES in the reaction of biodiesel production

Application	Process description	Results	Ref.
Purification of biodiesel	DES $K_2CO_3$ : glycerol = 1 : 4, ratio biodiesel to DES ratio of 1 : 4	Biodiesel purity = 98.724%	43
Purification of biodiesel (catalyst recovery)	Ternary DES ChCl : glycerol : ethylene glycol (2 : 1 : 2) & (1 : 2 : 2) DES : biodiesel (2.5 : 1)	Removal efficiency of KOH = 92.14%	49
Interesterification of lard	120 °C, 1 h, dosage = 0.9 g DES K–G/30 g (3 wt%) Biodiesel to DES K : G ratio 1 : 3	100% interesterification degree	35
Glycerol removal from biodiesel (microextractor)	DES choline chloride : ethylene glycol Biodiesel : DES ratio of 1 : 9 (v/v), extraction efficiency $T = 40$ °C, $\tau = 0.5$	Glycerol removal efficiency = 60.6%	37
Glycerol extraction from crude biodiesel	DES choline chloride–ethylene glycol (1 : 2.5, mol) Liquid–liquid extraction, DES to biodiesel mass ratio = 20%	FAME content = 98.55%	50
Biodiesel purification (extraction)	DES choline chloride : ethylene glycol (1 : 2) purification time = 30 min, DES : biodiesel (1 : 1)	Ester content = 96.96%	51



components.<sup>43</sup> In addition, due to its polarity, DES can also bind to KOH in biodiesel. This condition is attributed to the presence of hydroxyl groups in both DES and KOH in biodiesel, which enables DES to have a high ability to attract KOH through hydrogen bonding and dipole–dipole attraction. Additionally, DES has a high efficiency in separating glycerol from biodiesel, which is also due to its polarity, allowing it to form strong hydrogen bonds. In addition, the presence of hydroxyl groups in DES and glycerol, and the force to dissolve glycerol in biodiesel, resulted in a high ability for DES to attract glycerol through hydrogen bonding mechanisms and dipole–dipole interactions.<sup>44–46</sup>

Most studies focus on DES K–G either as a catalyst for transesterification or as a solvent for biodiesel purification separately. A detailed investigation into how DES K–G synergistically performs simultaneously in biodiesel production is still limited. The effects of DES characteristics, such as viscosity, polarity, and hydrogen bonding networks, on overall reaction kinetics and downstream purification efficiency when employed continuously or cyclically in biodiesel synthesis are not well understood.

The integration of DES K–G as a homogeneous catalyst, co-catalyst, and solvent in product purification still poses challenges due to its physical properties, and an optimum dose that is competitive with existing materials is yet to be determined. There is also limited information on how the DES K–G role affects the relevant biodiesel properties.

It is essential to gain a deeper understanding of the mechanistic aspects of the DES K–G, including its operation at the molecular and catalytic levels during transesterification, the effects of reaction medium and purification, as well as its interactions with glycerol and contaminants. This work will demonstrate the potential of DES K–G as a catalyst, reaction medium (co-catalyst), and washing solvent, utilizing simple applied technology without requiring extreme modifications to the existing biodiesel production system. Moreover, since DES K–G can be synthesized from materials available in the palm oil and biodiesel industry chain, the results of this research will enhance the efficiency and economics of sustainable biodiesel production, thereby contributing to a palm oil-based circular economy.

## 4 Materials and methods

### 4.1 Synthesis of DES K–G

The constituents of DES K–G in this study were industrial-grade glycerol and  $K_2CO_3$  with purities of 99.7% and 95%, respectively. Typically, both materials are mixed in a glass flask and further proceed in an incubator shaker at 80 °C for 3–4 hours, at a mixing speed of 400 rpm. The molar ratio of  $K_2CO_3$  to glycerol was 1 : 3.5. Previously,  $K_2CO_3$  was dehydrated in a vacuum oven for 2 hours at 150 °C.

The molar ratio  $K_2CO_3$ –glycerol, 1 : 3.5 corresponds to optimal performance in catalysis, extraction, or enzymatic processes. It gave the lowest-glycerol, fully liquid ratio, so it lies close to the practical eutectic region.<sup>52,53</sup>

### 4.2 Characterization of DES $K_2CO_3$ –glycerol

The physical–chemical properties of DES K–G observed include density, viscosity, freezing point, thermal conductivity, and pH. Brookfield Differential Scanning Calorimetry (DSC) was used to measure the freezing points of the DESs according to the ASTM D1177 method. Meanwhile, viscosity was measured using a rotational viscometer (a Brookfield DV-E). To identify functional groups and molecular interactions, such as hydrogen bonding, shifts in absorption bands were examined using Fourier Transform Infrared (FTIR) spectroscopy analysis. Nuclear Magnetic Resonance ( $^1H$ -NMR) spectroscopy was used to provide information on the structure and identity of the DES and the interactions between its components.

### 4.3 Transesterification (catalyst effectivity test)

The transesterification is carried out in a 500 mL 3-neck glass flask connected to a reflux condenser for methanol, a thermometer, and a sampler port. The raw material used was refined, bleached, deodorized palm oil (RBDPO) obtained from the oleochemical industry. Anhydrous methanol with a purity greater than 99.8% (Sigma Aldrich) was used in excess as a reactant. The molar ratio of methanol to palm oil was 8 : 1, or 30% by weight of palm oil. The catalyst was mixed with methanol, and then it was added to the palm oil to react at 65 °C, with

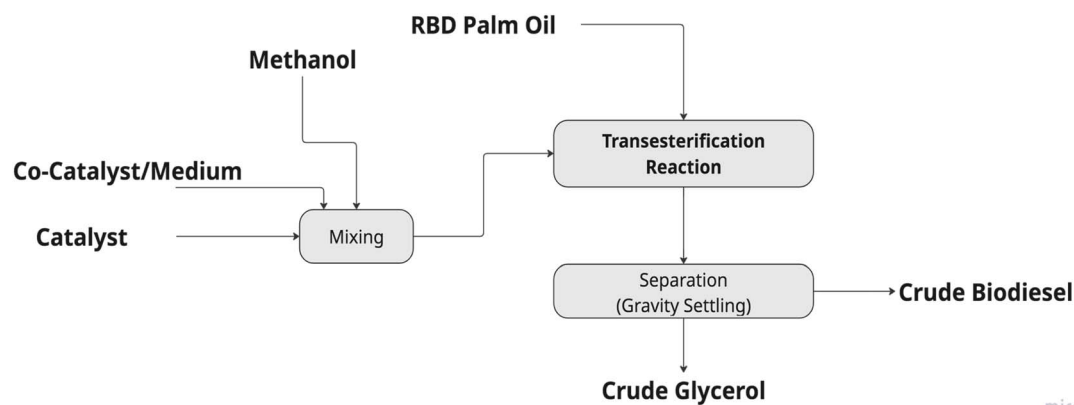


Fig. 1 Transesterification scheme for single and dual catalyst operations.



a stirring speed of 450 rpm. The complete process scheme is presented in Fig. 1.

In the dual-catalyst reaction system, the same apparatus and conditions were used. The variations in the volume ratio of SMO:DES K-G were 1:3, 1:1, and 3:1. The catalysts and co-catalysts/medium were first mixed in methanol, then added to the oil. The indicators of catalyst effectiveness were total glycerol, yield, and methyl ester content (MEC, %). Gas chromatography (GC-FID) was used to measure methyl ester content according to the standard test method as described in EN 14103.

#### 4.4 Biodiesel purification

The reaction mixture from the transesterification section was transferred to a separating funnel and separated into two phases: the top layer, which is crude biodiesel, and the lower layer, which is crude glycerol. Drain the glycerol layer (heavy phase) from the bottom valve or separatory funnel.

Crude Biodiesel (CB) was further subjected to purification stages through 1–2 cycles of washing using warm water and/or DES K-G, and a combination of both solvents, as shown in Fig. 2 and the treatment arrangement in Table 3.

In this study, CB washing was primarily conducted in two cycles (except for treatment 2) with a solvent-to-CB ratio of 1:1 (v/v). CB was mixed slowly with the solvent for 3–10 minutes, then allowed to settle for 60–120 minutes until the aqueous layer separated clearly. The parameters assessed as the most critical quality measures for purification assessment include methyl ester content, saponification value, acid value, and density. Some of the parameters that are considered critical for assessing purification effectiveness include methyl ester content (MEC), saponification value, acid value, and density. Saponification value (SV) refers to the amount of potassium hydroxide (KOH) in milligrams required to saponify one gram of fat or oil. It is an index of the average size of fatty acids present in the oil, which depends on the molecular weight and concentration of fatty acid components. According to the biodiesel standards (ASTM D6751 and EN 14214), the maximum SV of biodiesel is 312 mg KOH per g. While, Acid Value (AV)

Table 3 Biodiesel purification cycle arrangement

	Cycle 1		Cycle 2	
	Solvent	Vol ratio	Solvent	Vol ratio
Treatment 1	Water	1:1	Water	1:1
Treatment 2	DES K-G	1:1	—	—
Treatment 3	DES K-G	1:1	DES K-G	1:1
Treatment 4	DES K-G	1:1	Water	1:1
Treatment 5	Water	1:1	DES K-G	1:1

indicates the free fatty acid (FFA) content remaining in the biodiesel.

Separation efficiency ( $\eta$ ) quantifies how effectively unwanted substances are removed or valuable components are recovered. The separation efficiency value  $\eta$  of each parameter (density, AV, SV, MEC) with standards and methods as listed in Table 4 is calculated using the formula in eqn (1).

$$\eta = \frac{C_{\text{feed}} - C_{\text{product}}}{C_{\text{feed}}} \times 100\% \quad (1)$$

The biodiesel purification effectiveness then evaluated based on the changes in several parameters as listed in Table 4.

## 5 Results and discussion

### 5.1 The mechanism of DES K-G formation

The synthesis of DES K-G begins with the formation of carbonate anion ( $\text{CO}_3^{2-}$ ) as a base for releasing hydrogen ions

Table 4 Parameters of biodiesel purification effectiveness measurement

Parameter	Unit	Method	Standard
Saponification value	mg KOH per g	ASTM D5558	Max. 312
Density	kg m <sup>-3</sup>	ASTM D1298	860–900
Acid value	mg KOH per g	ASTM D664	Max. 0.50
Methyl ester content	% w/w	ASTM D7806	Min. 96.5%

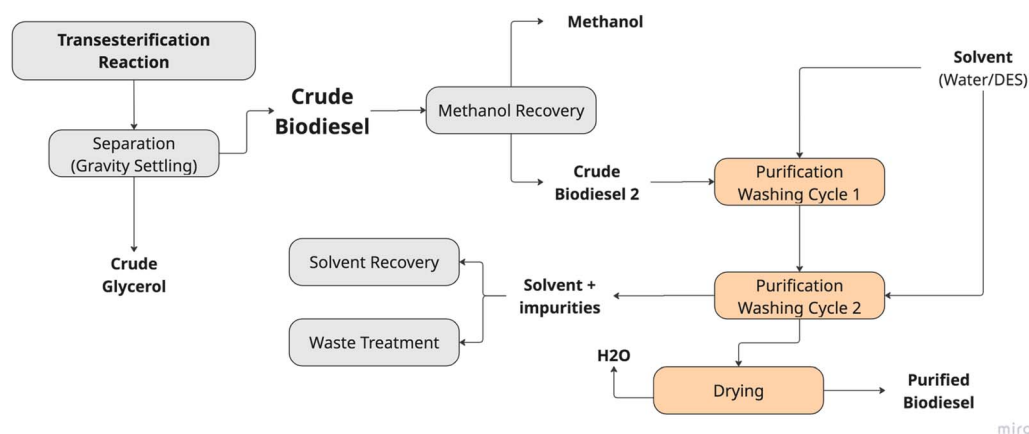


Fig. 2 Scheme of biodiesel purification.



( $H^+$  protons) from one of the hydroxy groups in glycerol. As presented in Fig. 3, the mechanism of DES K-G formation includes three stages: acid-base interaction, ionic network formation, and creation of the DES matrix through hydrogen bonding.

The molar ratio of  $K_2CO_3$  to glycerol was 1 : 3.5, which was considered an appropriate ratio to achieve the desired eutectic mixtures and a homogeneous DES structure. At this point, the composition between liquid glycerol and solid carbonate is in equilibrium. At this molar ratio, it is the first composition that forms a clear, homogeneous liquid with no undissolved salt. At this ratio, it provides sufficient  $K_2CO_3$  to maintain strong alkalinity and reactivity in the DES while ensuring complete dissolution, manageable viscosity, and ease of handling.<sup>54</sup> Conversely, at higher glycerol content, the hydrogen-bond network between the carbonate and the OH groups of glycerol is sufficient to keep everything in a single liquid phase.<sup>55</sup> Generally, eutectic reactions form characteristic microstructures, such as multiple layers or line patterns.

Multiple glycerol molecules interact with carbonate/bicarbonate and  $K^+$ , creating a dynamic hydrogen-bonded ionic lattice. A mixing temperature of 80 °C promoted the formation of the DES by increasing molecular mobility and facilitating the formation of hydrogen bonds. After 3–4 hours of mixing, the mixture of glycerol and carbonate ion formed a stable molecular network that governed DES formation as a homogeneous mixture.

The mechanism of DES formation involves a synergistic combination of partial proton transfer (from glycerol to carbonate), ion solvation, and hydrogen-bond network formation, which stabilises the liquid phase at temperatures significantly lower than those of the pure components.

The mechanism is essentially the disruption of the regular ionic lattice of  $K_2CO_3$  by strong directional hydrogen bonds from glycerol's hydroxyl groups, resulting in a stabilised eutectic mixture with unique fluid properties.

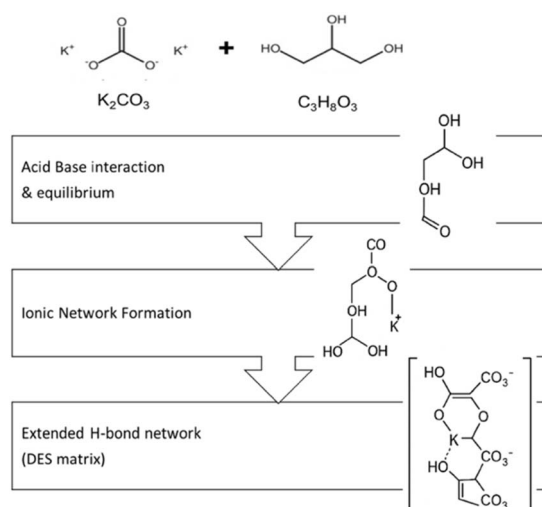


Fig. 3 Mechanism of DES K-G formation.



Fig. 4 DES  $K_2CO_3$ -glycerol.

## 5.2 Functional group and molecular structure

The analysis using Fourier transform infrared spectroscopy (FTIR) shows a shift in the stretching vibration of the  $-OH$  group of glycerol when mixed with  $K_2CO_3$ , indicating strong hydrogen bonding.

The electron cloud shift weakens the  $OH-$  bond, confirming the formation of hydrogen bonds between the hydroxyl groups of glycerol and the carbonate ions of potassium carbonate, due to a strong hydrogen bond network responsible for the eutectic behaviour, creating a highly viscous transparent base liquid considered as DES K-G, as shown in Fig. 4.

The IR spectrum of DES K-G confirms the extensive intermolecular hydrogen bonding and presence of carbonate functional groups in the  $K_2CO_3$ -glycerol mixture, which is consistent with typical deep eutectic solvent signatures. The presence of carbonate may shift and broaden some peaks, especially in the  $O-H$  and  $C-O$  regions, due to strong ionic or hydrogen-bonding interactions.

The broad and intense band around  $3174\text{ cm}^{-1}$  indicates a strong hydrogen bond interaction in glycerol mixed with  $K_2CO_3$ . A stronger hydrogen bond typically results in a broader and more shifted  $O-H$  peak toward lower wavenumbers due to the reduced bond energy in the  $OH$  group caused by hydrogen bonding.

As presented in Fig. 5 and Table 5, the  $C-H$  stretching is shown at  $2840\text{ cm}^{-1}$ , which is a typical characteristic of glycerol's alkyl groups. At  $1659\text{ cm}^{-1}$ , a peak was found that may be due to vibration modes associated with  $C=O$  or the bending of water. The water may be from absorbed moisture or hydrogen bonding in the DES. The water content of DES K-G presence can be inferred, especially from the broad  $O-H$  stretch region at  $3174\text{ cm}^{-1}$ .  $C-H$  bending or  $C-O$  stretching vibrations in glycerol have also been seen in  $1334\text{ cm}^{-1}$ .

The peaks at  $1111, 1039, 994, 923, 861\text{ cm}^{-1}$  are characteristic of  $C-O$  and  $C-C$  stretching and bending vibrations in glycerol. Vibrations of the carbonate ion can also influence peaks in this region. At the same time, a bending vibration is seen at  $670$  and  $509\text{ cm}^{-1}$ , which is possibly related to the carbonate ion ( $CO_3^{2-}$ ) group. The fingerprint region ( $<1500\text{ cm}^{-1}$ ) exhibits many overlapping bands characteristic of poly-alcohols, such as glycerol, with additional features from carbonate bending/stretching.



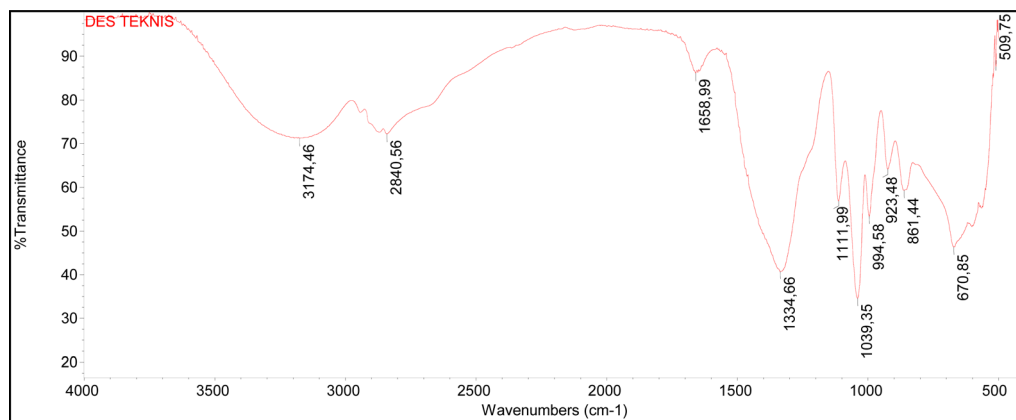


Fig. 5 IR spectrum of DES  $K_2CO_3$ - $C_3H_8O_3$ .

Table 5 The IR description for DES K-G

Wavenumber ( $cm^{-1}$ )	Assignment/functional group
3174	O-H stretch (hydrogen bonding)
2840	C-H stretch (glycerol)
1659	H-O-H bend, possible C=O env.
1334	C-O/H-C-O bending
1111-994	C-O stretch, finger-print of glycerol (and carbonate)
861-509	$CO_3^{2-}$ bending modes

Moreover, the peaks located at 1451, 1366, 1060, and 880  $cm^{-1}$  are assigned to the symmetric stretching vibration of C-O and the symmetric stretching vibration of C(-O)<sub>2</sub>. However, the formation of a new broad absorption band in the range of 3200-3500  $cm^{-1}$  is attributed to the stretching vibration of an intermolecular hydrogen bond, indicating the formation of weak interactions originating from hydrogen bonding between  $K_2CO_3$  and glycerol.

The functional group of DES K-G indicates the presence of hydrophilic or hydrophobic regions. The hydrophilic bands (O-H stretch) reveal strong hydrogen bonding and affinity for polar environments, while hydrophobic bands (C-H stretch) reveal the presence of nonpolar hydrocarbon regions, indicating the molecule's amphiphilic nature.

The presence of distinct chemical environments in the NMR spectrum, as shown in Fig. 5, indicates the formation of a eutectic mixture. H-NMR analysis was performed to confirm the spectral description related to DES K-G. Hydrogen bonds cause observable downfield shifts and changes in  $^1H$  NMR peak shapes, providing valuable insights into hydrogen bonding interactions in molecules.

When a hydrogen atom is involved in a hydrogen bond (-OH), its  $^1H$  NMR chemical shift typically moves downfield because the hydrogen nucleus becomes deshielded. It occurs due to a decrease in electron density around the proton caused by the interaction between the hydrogen on the hydroxyl group of glycerol and the oxygen on the carbonate.

Hydrogen-bonded protons often show broader signals due to exchange processes and dynamic hydrogen bonding. It can

exhibit a wide chemical shift range, often significantly downfield from non-hydrogen-bonded analogues. The chemical shift ranges from approximately 4.5 ppm to 19 ppm in strong hydrogen-bonded systems, as shown in Fig. 6.

In line with the report by Meng *et al.*,<sup>35</sup> the spectrum is dominated by glycerol signals (3.5-3.9 ppm). It supports the structural model in which coupling interaction occurs *via* the hydrogen bond between the -OH group of glycerol and the oxygen atoms of  $CO_3^{2-}$ . The proton signal peaks attributed to -CH<sub>2</sub>- are also diffused and gradually transformed into indistinguishable overlapping peaks. This pattern suggests that the more substantial impact of  $K_2CO_3$  and glycerol weakens the splitting of the  $^1H$  NMR resonance peaks caused by the induction effect.

### 5.3 The physicochemical properties

Molecular identification using H-NMR analysis and the functional groups of DES K-G confirms that the hydrogen bond network is the key factor influencing these physicochemical properties by modulating molecular mobility, phase behaviour, and ionic environment. Furthermore, some of the physicochemical properties of DES K-G are presented in Table 6.

The functional group of the DES K-G and the molecular structure, as indicated by the IR spectrum, are specifically affected by the type of protons present, their position, and the number of protons that produce signals of varying intensities. H NMR also provides valuable structural and dynamic insights that can be correlated with several physical properties of DES K-G.

The strong hydrogen bonding between  $K_2CO_3$  and glycerol decreased the melting/freezing point substantially compared to pure components as a eutectic effect. The strong H-bond and ionic interactions disrupt the regular lattice energy of  $K_2CO_3$ , preventing recrystallization. This condition is the defining feature of DESs, which shows a homogeneous form and remains liquid at room temperature.

In this work, DES K-G perform as an alkaline medium typically around pH 13-14. This condition is because  $K_2CO_3$  provides carbonate ions, which impart significant basicity to



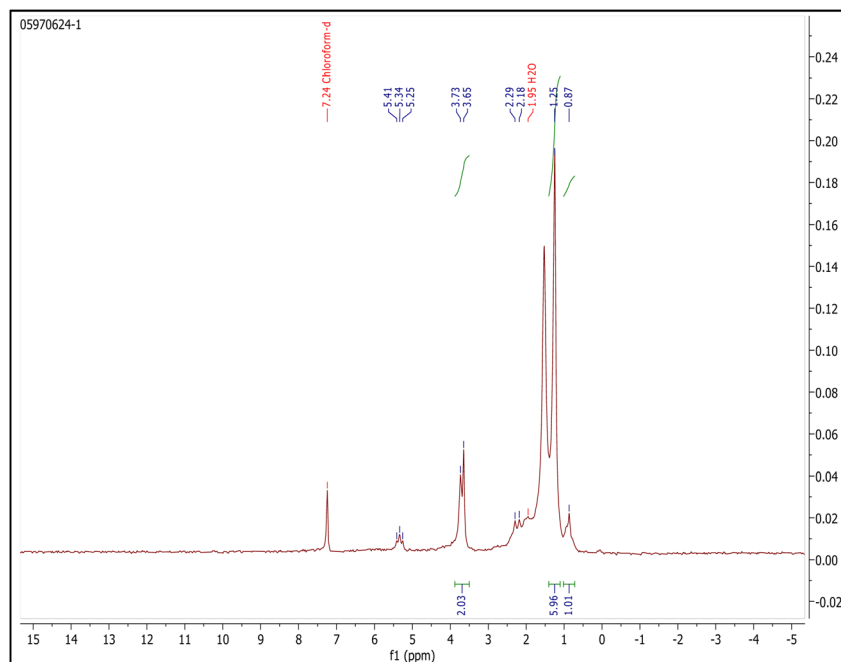


Fig. 6  $^1\text{H-NMR}$  of DES  $\text{K}_2\text{CO}_3$ -glycerol.

Table 6 DES K-G physical properties

Parameter	Units	DES $\text{K}_2\text{CO}_3$ -glycerol
Density	$\text{g cm}^{-3}$	16 302 (25 °C)
Viscosity	cP	70 785 (25 °C)
Conductivity	$\mu\text{S cm}^{-1}$	4612 (1% solution)
pH	—	13–14
Freezing point	°C	−9
Solubility	—	Soluble in water and methanol

the DES. The carbonate and glyceroxide anions act as Brønsted bases, consuming protons. The interaction with glycerol's hydroxyl groups stabilises the carbonate ions in the liquid DES phase, thereby ensuring a strongly alkaline environment.

The hydrogen bonds formed between the multiple hydroxyl groups of glycerol and carbonate ions create an extensive intermolecular network. The glycerol network forms dense intermolecular hydrogen bonds, while  $\text{K}^+$  ions coordinate to multiple oxygens. This cross-linking drastically reduces molecular mobility, resulting in a very high viscosity (70 785 cP).

A compact H-bonding and ion packing were well presented as seen in Fig. 5. Therefore, the small molecular size and strong hydrogen bonding lead to tight molecular packing, resulting in a higher density ( $1.63 \text{ g cm}^{-3}$ ). The presence of heavy  $\text{K}^+$  also contributes to the high density of DES K-G.

The conductivity properties of DES are related to the presence of cation ions ( $\text{K}^+$ ) and anions such as  $\text{CO}_3^{2-}$ ,  $\text{HCO}_3^-$ , or glycerolate ( $\text{C}_3\text{H}_7\text{O}_3^-$ ). All the ions are mobile inside the liquid because the DES forms a network of hydrogen bonds and solvates the ions, allowing them to move freely. The charge transport between ions refers to the movement of electric

charge through a medium, resulting in the high ionic conductivity of DES K-G ( $4612 \mu\text{S cm}^{-1}$ ). One of the most crucial properties for DES is the decrease in melting point. The formation of DES K-G in this study resulted in a significant depression of the freezing point by up to  $-9$  °C.

A decrease in the freezing points of the salts is due to their diminishing lattice energies, which allows the solid-liquid mixture to become liquid at ambient conditions.<sup>46</sup> The freezing points of ordinary, typical DESs depend on the hydrogen bond interaction and the salt/HBD molar ratio.<sup>56</sup>

$\text{K}_2\text{CO}_3$  can delocalize the charge through a hydrogen bonding network, thereby reducing the melting point and stabilizing the liquid state at lower temperatures. The determination of the ratio of moles  $\text{K}_2\text{CO}_3$  : glycerol = 1 : 3.5 proves that this mixing is near the eutectic composition. It gives the lowest freezing point, the most excellent ionic mobility, and optimum physicochemical balance (conductivity, viscosity, density).

#### 5.4 Catalytic activity

The catalytic performance of DES K-G was measured through tests on the transesterification reaction at a temperature of  $65$  °C, with a mole ratio of methanol to RBDPO of 8 : 1; the variables of the process carried out were catalyst loading (3–5%) and reaction time (1–4 hours). Tests on the same process conditions were also carried out using sodium methylate (SMO) catalysts. Due to the high viscosity of DES K-G, the addition of more methanol reduces the viscosity. It enhances contact between the polar methanol and the catalyst, as well as non-polar phases of palm oil, thereby improving the rate.

The results of the transesterification test with DES K-G as a catalyst on the variation of catalyst loading and reaction time are shown in Fig. 7. From this, it is confirmed that DES K-G can act as



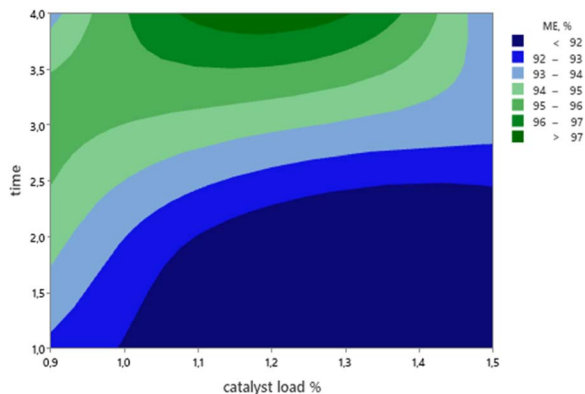


Fig. 7 Catalytic performance of DES K-G with variation of catalyst loading and reaction time.

a catalyst in the transesterification reaction of palm oil to produce biodiesel that meets both SNI and ASTM quality standards. The use of DES K-G as a catalyst shows that the yield is between 95% and 102%, while the methyl ester content has reached or exceeded the minimum standard of biodiesel quality (>96.5%).

The catalytic properties of DES K-G are dominant due to the presence of  $K_2CO_3$  and its interaction with glycerol. In DES,  $K_2CO_3$  becomes activated where carbonate ions and potassium cations are solvated by glycerol, forming potassium glycerolates and bicarbonate-like basic centres. Due to its excellent mobility and strong basicity, both ionic species can effectively abstract protons to create the active methoxide nucleophile. Strong basic species, such as methoxides, are formed when glycerol stabilises carbonate anions.

DES reduces viscosity mismatch between polar methanol and nonpolar oil, acting as a phase-transfer medium in the transesterification process. The carbonate ions are fully solvated, which means more active sites are available than in solid  $K_2CO_3$ .

The formation of the DES K-G complex activates the hydroxyl oxygen of the glycerol. This activated alcohol is crucial because it is more favourable to attack the positive carbon of the carbonyl group, which is coordinated with  $K^+$ , during the transesterification process, thereby increasing the catalytic efficiency.

DES K-G provides high basicity, allowing  $K_2CO_3$  to facilitate the formation of methoxide.  $K_2CO_3$  in DES is converted into potassium glyceroxide/alkoxide ( $K-O^-$ ) species. These species deprotonate methanol to give  $K^+-OCH_3$  (methoxide), which performs the nucleophilic attack on triglyceride carbonyls, forming a tetrahedral intermediate, which collapses to one molecule of fatty acid methyl ester (FAME), and the corresponding diglyceride. Afterward, the glycerol-rich, ionic environment of the DES stabilizes active K species and enhances miscibility with methanol and oil, making DES  $K_2CO_3$ -glycerol an efficient liquid base catalyst for palm-oil transesterification.  $K^+/CO_3^{2-}$  are present in the liquid reaction medium rather than confined to a solid surface. K species leach from  $K_2CO_3$  into the reaction medium, which is intrinsic to carbonate-catalyzed transesterification and is enhanced by glycerol.<sup>57,58</sup>

Glycerol in DES acts as a hydrogen bond donor, stabilising the catalyst system and potentially enhancing substrate accessibility. The DES environment maintains ions *via* hydrogen bonding from glycerol. The strong hydrogen bonding that causes the freezing point depression also creates stable reactive intermediates, such as methoxide or diglyceride ions. It also creates a polar environment that facilitates the transesterification process. The high conductivity of DES K-G correlates with its ability to help proton abstraction, methoxide formation, and regeneration of catalyst sites. The high conductivity also enhances reactivity, where DES improves contact between oil and methanol in the transesterification process.

As with the reaction mechanism that occurs with sodium or potassium methylate catalysts, DES generates a reactive methoxide ion that promotes the nucleophilic substitution on triglycerides, efficiently producing fatty acid methyl ester.  $K_2CO_3$  and glycerol form basic potassium glycerolate-like species, which deprotonate methanol to methoxide ( $CH_3O^-$ ), which attacks triglyceride carbonyls, forming methyl esters and glycerol in the usual transesterification pathway. The DES matrix stabilizes ionic species and increases local base concentration.<sup>14</sup>

The presence of DES K-G in the reaction successfully lowers the activation energy, which is triggered by the ionic properties of the medium. It facilitates the nucleophilic attack of alcohols on carbonyl triglyceride groups. The ionic atmosphere it generates enables efficient molecular collisions, allowing reactions to occur at lower temperatures than conventional catalytic systems. Under the same process conditions and catalyst ratio, the effect of DES K-G as a transesterification catalyst for palm oil is compared to that of a commercial catalyst, namely sodium methylate.

As shown in Fig. 8, it is confirmed that to produce a methyl ester product meeting the same quality standards, the transesterification reaction with the DES K-G catalyst requires a longer reaction time (4 h). In contrast, the SMO catalyst requires less than two hours. However, with yield and product purity that both meet quality standards, it proves that DES K-G has the ability equivalent to SMO catalysts to achieve thermodynamic equilibrium, albeit with slower kinetics.

The thermodynamic equilibrium related to the methoxide production rate of DES-KG was slower than that of SMO. DES K-G acts as a basic catalyst *via* the carbonate ion, which deprotonates methanol to form methoxide ions, but in a less

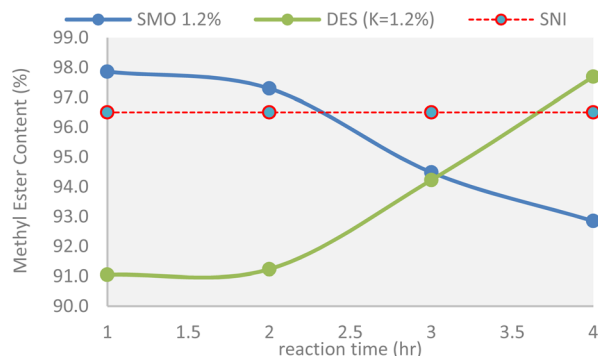


Fig. 8 The performance of DES K-G and SMO catalysts on catalyst loading variations and reaction times.



aggressive manner than sodium methoxide. Otherwise, sodium methoxide provides a more immediate and substantial basic environment, yielding faster reaction rates but with increased side reactions and handling complexity.

### 5.5 Performance in dual catalyst system

Applying a dual catalyst system that combines sodium methoxide and DES K-G in transesterification can potentially leverage the advantages of both catalysts mechanistically while altering reaction dynamics. Combining catalysts can create synergistic effects that improve activity and stability compared to using single catalysts. Hybrid catalysts show improved performance, reducing catalyst usage while sustaining high conversion rates.

In this dual catalyst setup, either SMO or DES K-G was pre-mixed with methanol to form a catalyst-methanol solution. Both catalysts were dissolved or dispersed in methanol to create a uniform catalytic solution, which was then mixed with the oil feedstock. This condition ensures that both catalysts are fully activated and evenly distributed for simultaneous action. A medium stirring of 200 rpm was applied to maximise catalyst interaction. The reaction condition was set the same as in the previous test, while the total loading of catalyst for each test was 1.2% w/w of palm oil.

The weight fraction of DES in a mixture with SMO varies from 25%, 50%, and 75% (or weight ratios of 1 : 3, 1 : 1 and 1 : 0.33). The transesterification process is carried out at a time variation of 1–4 hours. The results of the transesterification process test using a dual catalyst (DES, KG, and SMO) are shown in Fig. 9.

The fraction of SMO is set higher than that of DES K-G in a dual-catalyst system to achieve higher methyl ester content. SMO could provide a hybrid catalytic environment where the stabilising complement complements fast methoxide generation from sodium methoxide. In contrast, the less aggressive catalytic action of the DES balances reaction speed and controls side reactions. The dual catalysis system has shown improvements in biodiesel yield and purity, while offering more robust catalytic performance compared to either catalyst alone.

In a catalyst mixture with SMO, DES K-G acts as a reaction medium that enhances the solubility of both the triglyceride and

the methanol phases. By creating a homogeneous reaction environment, DES K-G facilitates the interaction between oil and methanol, thereby accelerating the reaction. Dual catalyst use correlates with potentially shorter reaction times than DES alone, due to enhanced initial catalytic activity; however, overall kinetics are modulated to reduce side reactions through the milder DES influence.

To obtain methyl ester levels that meet the minimum quality standard of FAME greater than 96%, a 1 : 1 mixing ratio between DES and SMO can be achieved in a reaction time of 2–3 h. In comparison, higher methyl ester levels of up to 98% can be obtained by increasing the SMO fraction and using 25% DES; the reaction time can be reduced to less than 2 h.

The combination of SMO and DKG can accelerate the initial reaction rate due to the rapid generation of methoxide ions by sodium methoxide, thereby reducing the minimum reaction time required. The DES component can stabilise the reaction environment, potentially extending effective catalytic activity and reducing side reaction rates over longer reaction periods.

### 5.6 Performance in biodiesel purification

The result of the transesterification reaction formed two layers consisting of crude biodiesel (CB) and crude glycerol (CG). In this section, the focus of the separation effectiveness test using DES-KG is on the top biodiesel phase obtained from separation with the principle of gravity settling.

Before entering the purification stage, utilising the water and solvent washing technique, the methanol is first separated using flash evaporation at 60–70 °C. In addition to methanol residues, CB generally contains various impurities such as soaps, FFAs, and residual glycerides.

The results of the biodiesel purification test are presented in Table 7. It was found that treating with DES K-G as a washing medium in one cycle yielded better results than washing with water in two cycles. The DES-treated biodiesel in a single washing cycle provided a higher methyl ester content comparable to that of samples washed with water for two cycles. Moreover, all treatments using DES K-G showed noticeable/changes in density, SV, AV, and MEC compared to washing with water.

As seen on Table 7, DES plays a significant role in the biodiesel washing process. This achievement is mainly due to biodiesel being less dense and nonpolar relative to DES K-G and water. DES K-G acts as a polar solvent, extracting residual methanol, soap, and catalyst, as well as small polar glycerol traces. After the CB was washed with DES K-G, a distinct solvent-rich layer containing these impurities can form, separated from the biodiesel. Between or beneath these layers, impurities such as glycerol, soaps, unreacted oils, free fatty acids, methanol, and water contaminants tend to accumulate.

The layers formed typically resemble a biphasic system, where the upper layer is the purified biodiesel and the lower, dense, viscous layer is the DES with concentrated impurities.

Meanwhile, glycerol as a hydrogen donor provides high polarity to attract contaminants without forming persistent emulsions. The stability of the product, attributed to the

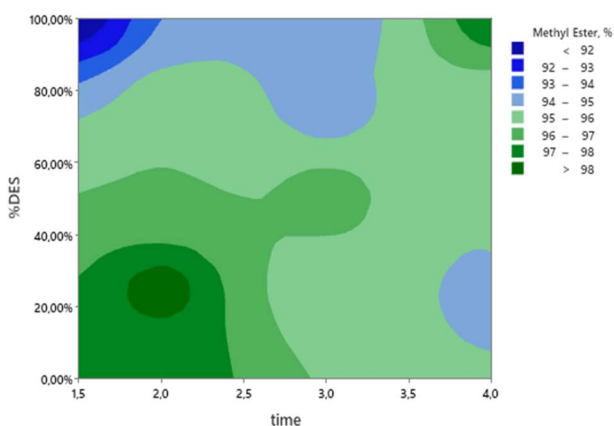


Fig. 9 Performance of DES as co-catalyst (with SMO) in transesterification reactions.



Table 7 Results of crude biodiesel washing with water and/or DES K-G

Treatment	Solvent used in CB washing		Density, kg m <sup>-3</sup>	Saponification value, mg KOH per g	Acid value, mg KOH per g	Methyl ester content (%)
	Cycle 1	Cycle 2				
	Initial		866.740	213.543	0.383	93.277
1	Water	Water	867.885	198.024	0.328	95.404
2	DES K-G	—	870.342	189.413	0.298	97.105
3	DES K-G	DES K-G	877.323	181.719	0.282	98.116
4	DES K-G	Water	876.705	183.024	0.201	98.256
5	Water	DES K-G	876.963	186.024	0.218	97.718

presence of glycerol in DES, has been demonstrated to prevent soap formation and is supported by a decrease in SV.

As seen in Fig. 10 and 11, CB washing involving DES K-G or a combination of water and DES K-G (treatment 3, 4, and 5) provides better purification effectiveness, as indicated by the percentage change (increase) in density and methyl ester content, and the decrease in saponification value and acid value.

DES K-G improves phase separation by disrupting emulsion stability. Therefore, washing with DES K-G tends to result in higher methyl ester levels. Continuing the washing stage with water in the second cycle clearly improves the process by

reducing contaminated water and utilising the solvent DES in a lower volume ratio (1 : 1) for optimal purification results.

The increase in biodiesel density after may be due to excessive DES mixing doses, causing glycerol in DES to be entrained in biodiesel. DES can also preferentially extract lighter components (residual alcohol, light esters), leaving a heavier average FAME profile that slightly increases density. This statement has also been reported by Mishra *et al.*<sup>59</sup> and Mamtani *et al.*<sup>16</sup>

DES K<sub>2</sub>CO<sub>3</sub>-glycerol is so polar and dense that any carry-over or glycerol retention in biodiesel will increase the measured density, even though GC may show higher methyl ester content (ester purity). If phase separation is not perfectly conducted,

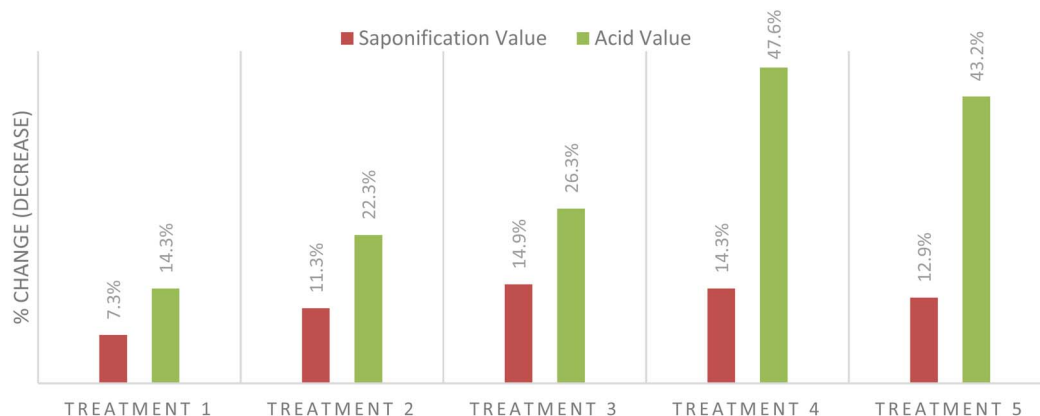


Fig. 10 Effects of crude biodiesel treatment to saponification value and acid value.

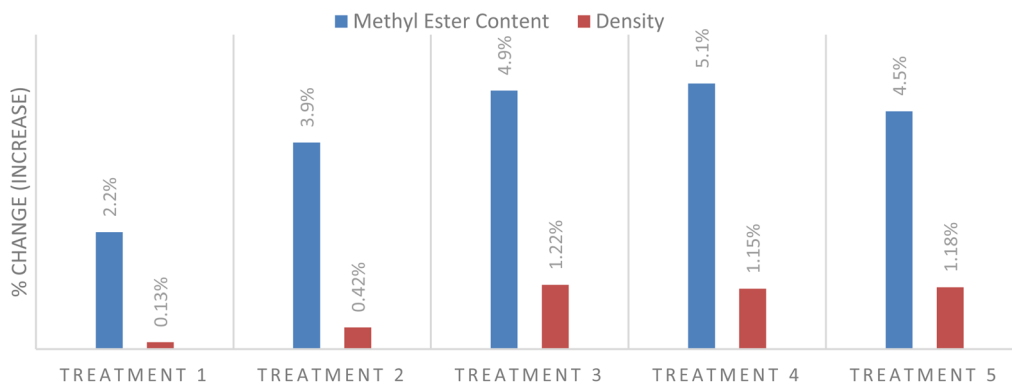


Fig. 11 Effects of crude biodiesel treatment to density and methyl ester content.



small amounts of DES can remain dispersed in the biodiesel phase. A DES-rich microemulsion will increase the bulk density of the biodiesel.

## 6 Conclusions

Under process conditions commonly applied in biodiesel plants and the same catalyst ratio, DES K-G has shown effective catalytic activity in transesterification, as well as commercial catalysts (sodium methylate), even requiring extra reaction time (4 h). In a dual-catalyst system, the addition of 25% DES (SMO : DES ratio = 3 : 1) to the mixture with SMO successfully yields a 98.6% methyl ester content and reduces the reaction time to less than 120 minutes. Notably, the use of DES has significantly shortened the reaction time required to meet biodiesel standards, demonstrating improved efficiency. Furthermore, as a solvent, DES K-G has demonstrated superior performance in biodiesel washing. The key performance indicators, including a decrease in saponification and acid values, alongside an increase in methyl ester content and density, confirm the efficacy of DES K-G. The combination of 2-cycle biodiesel washing with DES K-G in the first cycle and water in the second cycle, with a ratio of CB : DES K-G (1 : 1) and CB : water (1 : 1), resulted in an average impurity removal efficiency of 17.02%. DES K-G is a potentially sustainable and effective alternative to water or dry-wash purification systems for biodiesel and could be successfully adopted in both current and future production settings.

These findings highlight not only the potential of DES K-G to enhance biodiesel production but also its role in improving product quality. The multifunctionality of DES K-G as both a catalyst, reaction medium and solvent represents a promising advancement, paving the way for more sustainable and efficient biodiesel production methods. Further research will explore the scalability of the experiment, aiming to find the optimal conditions for fully integrating DES K-G in biodiesel production that can be compatible and industrial-level validated in the future.

## Author contributions

Leily Nurul Komariah: conceptualization; methodology; supervision; formal analysis; writing – original draft, validation, Susila Arita: supervision; funding acquisition, M. D. Khairuddin: investigation; data curation, S. A. Ovindirani: investigation; data curation, Desi Erisna: project administration; data curation, Tsabita N. Paramasyifa: writing – review & editing, visualization.

## Conflicts of interest

There are no conflicts of interest to declare.

## Data availability

The data that support the findings of this study are available from the corresponding author upon reasonable request.

## Acknowledgements

We acknowledge the Oil Palm Plantation Fund Management Agency of the Ministry of Finance of the Republic of Indonesia (BPDPKS), which funded this research. In particular, the authors would like to express their gratitude to Dr Tatang Hernas Soerawidjaja (ITB) for his inspiration and the technical guidances.

## Notes and references

- 1 L. N. Komariah, *RSC Adv.*, 2024, **14**, 6112–6120.
- 2 N. E. Benti, A. B. Aneseyee, C. A. Geffe, T. A. Woldegiyorgis, G. S. Gurmesa, M. Bibiso, A. A. Asfaw, A. W. Milki and Y. S. Mekonnen, *Sci. Afr.*, 2023, **19**, e01531.
- 3 B. Wang, B. Wang, S. K. Shukla and R. Wang, *Catalysts*, 2023, **13**, 1–23.
- 4 A. A. Babadi, S. Rahmati, R. Fakhlaei, B. Barati, S. Wang, W. Doherty and K. Ostrikov, *Biomass Bioenergy*, 2022, **163**, 106521.
- 5 V. P. Indran, A. S. Haji Saud, G. P. Maniam, M. M. Yusoff, Y. H. Taufiq-Yap and M. H. Mohd, *RSC Adv.*, 2016, **6**, 411.
- 6 D. Singh, P. K. Sharma, A. Pawar and S. S. Godara, *Sci. Rep.*, 2025, **15**, 41781.
- 7 I. Ridwan, H. Budiastuti, R. Indarti, N. L. E. Wahyuni, H. M. Safitri and R. L. Ramadhan, *Mater. Sci. Energy Technol.*, 2023, **6**, 15–20.
- 8 W. Songoen, V. Punsuvon, W. Arirop and A. Timyamprasert, *Appl. Mech. Mater.*, 2018, **876**, 9–14.
- 9 I. M. Atadashi, *Alexandria Eng. J.*, 2015, **54**, 1265–1272.
- 10 W. Limmun and S. Sansiribhan, *E3S Web Conf.*, 2020, **187**, 1–8.
- 11 N. E. Rodriguez and M. A. Martinello, *Fuel*, 2021, **296**, 120597.
- 12 H. Bateni, A. Saraeian and C. Able, *Biofuel Res. J.*, 2017, **4**, 668–690.
- 13 V. Sharma, *Bioresour. Technol.*, 2022, **360**, 127631.
- 14 E. L. Smith, A. P. Abbott and K. S. Ryder, *Chem. Rev.*, 2014, **114**, 11060–11082.
- 15 L. Zhang, Y. Li, R. Li, H. Yu, S. Yang, M. Ding and H. Xie, *Bioresour. Technol.*, 2026, **439**, 133271.
- 16 K. Mamtani, K. Shahbaz and M. M. Farid, *Fuel*, 2021, **295**, 120604.
- 17 B. B. Hansen, S. Spittle, B. Chen, D. Poe, Y. Zhang, J. M. Klein, A. Horton, L. Adhikari, T. Zelovich, B. W. Doherty, B. Gurkan, E. J. Maginn, A. Ragauskas, M. Dadmun, T. A. Zawodzinski, G. A. Baker, M. E. Tuckerman, R. F. Savinell and J. R. Sangoro, *Chem. Rev.*, 2021, **121**, 1232–1285.
- 18 M. A. R. Martins, S. P. Pinho and J. A. P. Coutinho, *J. Solution Chem.*, 2019, **48**, 962–982.
- 19 L. Duan, S. Han, Z. Zhang, J. Xu, D. Wang, S. Chen, J. Wang, J. Lv, C. Guo and Y. Li, *Bioresour. Technol.*, 2026, **442**, 133738.
- 20 Y. A. Salam, L. N. Komariah, F. Hadiyah and S. Arita, *Science and Technology Indonesia*, 2024, **9**, 28–35.
- 21 M. Sung and J. I. Han, *Bioresour. Technol.*, 2016, **205**, 250–253.
- 22 K. Malins, *Fuel Process. Technol.*, 2018, **179**, 302–312.



- 23 E. G. Silveira Junior, V. H. Perez, I. Reyero, A. Serrano-Lotina and O. R. Justo, *Fuel*, 2019, **241**, 311–318.
- 24 C. Baroi, E. K. Yanful and M. A. Bergougnou, *Int. J. Chem. React. Eng.*, 2009, **7**, 1–13.
- 25 R. Shan, J. Shi, B. Yan, G. Chen, J. Yao and C. Liu, *Energy Convers. Manage.*, 2016, **116**, 142–149.
- 26 M. Z. Salmasi, M. Kazemeini and S. Sadjadi, *Ind. Crops Prod.*, 2020, **156**, 112846.
- 27 A. H. Mohammad Fauzi and N. A. S. Amin, *Renewable Sustainable Energy Rev.*, 2012, **16**, 5770–5786.
- 28 A. Ranjan, S. S. Dawn, N. Nirmala, A. Santhosh and J. Arun, *Fuel*, 2022, **307**, 121933.
- 29 D. Z. Troter, Z. B. Todorović, D. R. Dokić-Stojanović, O. S. Stamenković and V. B. Veljković, *Renewable Sustainable Energy Rev.*, 2016, **61**, 473–500.
- 30 M. A. Alam, L. Deng, A. D. P. Ngatcha, A. D. T. Fouegue, J. Wu, S. Zhang, A. Zhao, W. Xiong and J. Xu, *Ind. Crops Prod.*, 2023, **206**, 117725.
- 31 S. Arita, L. N. Komariah, W. Andalia, F. Hadiah and C. Ramayanti, *Emerging Science Journal*, 2023, **7**, 917–927.
- 32 Q. Liu, M. Wang, Z. Jiang, G. Yang, J. Wei and T. Fang, *Chem. Eng. J.*, 2018, **349**, 192–203.
- 33 K. Mamtani, K. Shahbaz and M. M. Farid, *Fuel*, 2021, **295**, 120604.
- 34 Z. B. Todorović, B. S. Đorđević, D. Z. Troter, L. M. Veselinović, M. V. Zdujić and V. B. Veljković, *Hem. Ind.*, 2023, **77**, D1.
- 35 P. Meng, J. Li, W. Liu, G. Yang, R. Yang, S. Liang and C. Sun, *Lwt*, 2023, **186**, 115232.
- 36 S. T. Williamson, K. Shahbaz, F. S. Mjalli, I. M. AlNashef and M. M. Farid, *Renewable Energy*, 2017, **114**, 480–488.
- 37 S. Anđelović, M. Božinović, Ž. Čurić, A. Šalić, A. Jurinjak Tušek, K. Z. Kučan, M. Rogošić, M. Radović, M. Cvjetko Bubalo and B. Zelić, *Bioengineering*, 2022, **9**, 1–21.
- 38 T. Homan, K. Shahbaz and M. M. Farid, *Sep. Purif. Technol.*, 2017, **174**, 570–576.
- 39 Q. Zhang, K. De Oliveira Vigier, S. Royer and F. Jérôme, *Chem. Soc. Rev.*, 2012, **41**, 7108–7146.
- 40 A. Sander, A. Petračić, J. P. Vuković and L. Husinec, *Separations*, 2020, **7**, 1–18.
- 41 A. A. M. Lapis, L. F. De Oliveira, B. A. D. Neto and J. Dupont, *ChemSusChem*, 2008, **1**, 759–762.
- 42 L. Gu, W. Huang, S. Tang, S. Tian and X. Zhang, *Chem. Eng. J.*, 2015, **259**, 647–652.
- 43 R. Manurung, A. Arief and G. R. Hutauruk, *AIP Conf. Proc.*, 2018, **1977**, 0200101–0200108.
- 44 H. Ghaedi, M. Ayoub, S. Sufian, A. M. Shariff and B. Lal, *Preprints*, 2017, pp. 1–25, DOI: [10.20944/preprints201705.0148.v1](https://doi.org/10.20944/preprints201705.0148.v1).
- 45 W. Liu and F. Wang, *J. Oleo Sci.*, 2018, **67**, 1163–1169.
- 46 Y. Marcus, in *Deep Eutectic Solvents*, 2019, pp. 1–44.
- 47 A. Abdurrahman, S. M. Waziri, O. A. Ajayi and F. N. Dabai, *Journal of the Nigerian Society of Physical Sciences*, 2023, **5**, 1–9.
- 48 W. Huang, S. Tang, H. Zhao and S. Tian, *Ind. Eng. Chem. Res.*, 2013, **52**, 11943–11947.
- 49 P. Hui Min, K. Shahbaz, W. Rashmi, F. S. Mjalli, M. A. Hashim and I. M. Alnashef, *Journal of Engineering Science and Technology*, 2015, **10**, 35–49.
- 50 A. Sander, A. Petračić, D. Vrsaljko, J. Parlov Vuković, P. Hršak and A. Jelavić, *Separations*, 2024, **11**, 1–16.
- 51 M. Khanian-Najaf-Abadi, B. Ghobadian, M. Dehghani-Soufi and A. Heydari, *Biomass Convers. Biorefin.*, 2024, **14**, 8469–8481.
- 52 H. Wang, T. Liu, C. Jiang, Y. Wang and J. Ma, *Chem. Eng. J.*, 2022, **442**, 1–21.
- 53 J. Naser, F. Mjalli, B. Jibril, S. Al-Hatmi and Z. Gano, *Int. J. Chem. Eng. Appl.*, 2013, **4**, 114–118.
- 54 F. S. Mjalli, J. Naser, B. Jibril, S. S. Al-Hatmi and Z. S. Gano, *Thermochim. Acta*, 2014, **575**, 135–143.
- 55 R. Li, P. H. Hsueh, S. A. Ulfadillah, S. T. Wang and M. L. Tsai, *Polymers*, 2024, **16**, 3187.
- 56 D. J. Ramon and G. Guillena, *Deep Eutectic Solvents Synthesis, Properties, and Applications*, Wiley-VCH Verlag, 2020.
- 57 L. Čapek, M. Hájek, P. Kutálek and L. Smoláková, *Fuel*, 2014, **115**, 443–451.
- 58 M. Nyepetsi, F. Mbaiwa, O. A. Oyetunji, N. Y. Dzade and N. H. de Leeuw, *S. Afr. J. Chem.*, 2021, **74**, 42–49.
- 59 S. Mishra, K. R. Bukkarapu and A. Krishnasamy, *Fuel*, 2021, **285**, 1–17.

